Chapter 3

Experimentation

3.1 Introduction

This chapter includes the design and experimental analysis of parabolic trough concentrator system. A fundamental relation has been developed between aperture and receiver area using a simple mathematical approach. Emphasis are given to three major parameters: geometric concentration ratio, acceptance angle and rim angle that are essential to design concentrating collectors. Among the three parameters, the concentration ratio is the most important. It represents the ratio of aperture area to the receiver area. According to the second law of thermodynamics applied to the solar radiation heat exchange between the sun and the receiver, the maximum value of concentration ratio obtained for parabolic trough collector is 212 [142]. The acceptance angle represents the angular range over which all direct reflected solar rays by the collector reaches the absorber tube when the system is well focused. The third most important parameter is the Rim angle for designing the parabolic trough concentrator. It links the three other parameters of the PTCs like arc length, focal length and aperture width of the collector [143] as shown in figure 3.1. This chapter also includes the experimental analysis: description of experimental setup, instrumentation, geometry and designed dimensions.

3.2 Mathematical Analysis of solar collectors

3.2.1 Assumptions

Following are the assumptions for designing a parabolic trough collector for improving collection efficiency:

- Total solar radiation after reflection from the aperture is intercepted by receiver at

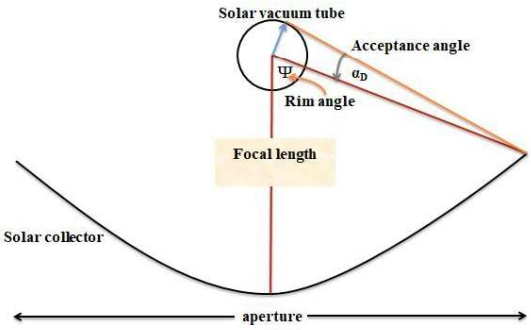

Figure 3.1: Basic design angles

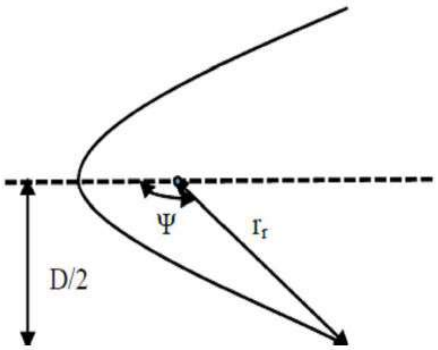

Figure 3.2: Aperture parameters

the focus (intercept factor is 1).

- No portion of aperture area of a parabolic trough concentrator is shaded by the receiver.
- Solar radiation falls on the aperture is constant.

From right angled triangle, as shown in figure (3.3)

$$\frac{d}{2} = r_r \sin(\alpha_D/2) \tag{3.1}$$

$$d = 2\,r_r \sin(\alpha_D/2) \tag{3.2}$$

Where,

$D = aperture\,diameter$

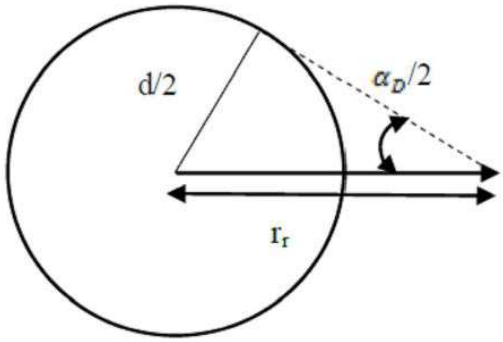

Figure 3.3: Receiver parameters

$d = absorber\,diameter,$

$\alpha_D = sun\,beam\,angle, (32\,minutes)$

$r_r = distance\,between\,the\,absorber\,tube\,and\,the\,mirror\,rim,$

$\Psi = Rim\,angle$

$h = depth\,of\,parabola$

Alternatively it can be written r_r in terms of D and Ψ

$$r_r = \frac{D}{2\sin\Psi} \tag{3.3}$$

From (3.2) and (3.3) it can be concluded that,

$$d = \frac{D}{\sin\Psi}\sin(\alpha_D/2) \tag{3.4}$$

Rim angle can be expressed in terms of d and h

$$\tan\Psi_{rim} = \frac{1}{\frac{d}{8h} + \frac{2h}{d}} \tag{3.5}$$

$$\tan\Psi_{rim} = \frac{\frac{f}{d}}{2\left(\frac{f}{d}\right)^2 - \frac{1}{8}} \tag{3.6}$$

Relationship between$h$, f & D

$$h = \frac{D^2}{16f} \tag{3.7}$$

Now the arc length of parabolic trough can be calculated as, The general formula for calculating arc length of a parabola is as under;

Equation of parabola:

$$y^2 = 4fx \tag{3.8}$$

So,

$$x = \frac{y^2}{4f} \tag{3.9}$$

or it can also be written as;

$$f(y) = \frac{y^2}{4f} \tag{3.10}$$

Differentiating it with respect to y

$$f'(y) = \frac{y}{2f} \tag{3.11}$$

The general formula for arc length

$$s = \int_{y_1}^{y_2} \sqrt{1 + \left(f'(y)\right)^2}\, dy \tag{3.12}$$

here limits are $y_1 = -D/2$ & $y_2 = +D/2$

$$s = \int_{-D/2}^{+D/2} \sqrt{1 + \left(f'(y)\right)^2}\, dy \tag{3.13}$$

Therefore, after integration,

$$s = \frac{D}{2}\sqrt{1 + \frac{D^2}{16f^2}} + 2f \ln\left(\frac{D}{4f} + \sqrt{1 + \frac{D^2}{16f^2}}\right) \tag{3.14}$$

Now from equation (3.7) $h = \frac{D^2}{16f}$

So from this relation, arc length in terms of f and D;

$$\frac{4h}{D} = \frac{D}{4f}$$

so,

$$s = \frac{D}{2}\sqrt{1+\left(\frac{4h}{D}\right)^2} + 2f\ln\left(\frac{4h}{D} + \sqrt{1+\left(\frac{4h}{D}\right)^2}\right) \tag{3.15}$$

The area of parabolic trough aperture as follows

$$A_a = S \times L \tag{3.16}$$

Where L is the length of the parabolic trough and s is the arc length. The area of cylindrical absorber can be calculated as follows;

$$A_r = \pi d L \tag{3.17}$$

So concentration ratio ($C.R.$) as per definition

$$CR = \frac{A_a}{A_r} \tag{3.18}$$

After putting the values of A_a and A_r

$$CR = \frac{s}{\pi d}$$

$$\frac{A_a}{A_r} = \frac{s}{\pi d}$$

$$A_a = \frac{s}{\pi d} A_r$$

Now from the equation (3.15)

$$A_a = \frac{\frac{D}{2}\sqrt{1+\left(\frac{4h}{D}\right)^2} + 2f\ln\left(\frac{4h}{D} + \sqrt{1+\left(\frac{4h}{D}\right)^2}\right)}{\pi d} A_r \tag{3.19}$$

Now from equation (3.4),

$$d = \frac{D}{\sin\Psi}\sin\left(\frac{\alpha_D}{2}\right)$$

Where α_D =sun beam angle, (32 minutes) After putting value of ,

$$d = \frac{D}{\sin\Psi}(0.004654)$$

Now putting this value of d in equation (3.19)

$$A_a = \frac{\frac{D}{2}\sqrt{1+\left(\frac{4h}{D}\right)^2}+2f\ln\left(\frac{4h}{D}+\sqrt{1+\left(\frac{4h}{D}\right)^2}\right)}{\pi\frac{D}{\sin\Psi}(0.004654)}A_r$$

$$A_a = \frac{\sin\Psi\left[\frac{1}{2}\sqrt{1+\left(\frac{4h}{D}\right)^2}+\frac{2f}{D}\ln\left(\frac{4h}{D}+\sqrt{1+\left(\frac{4h}{D}\right)^2}\right)\right]}{(0.1461417)}A_r$$

$$A_a = \frac{\sin\Psi}{D}\left[34.2133\sqrt{D^2+16h^2}+136.8534f\ln\left(\frac{4h+\sqrt{D^2+16h^2}}{D}\right)\right]\times A_r \quad (3.20)$$

Now from equation (7) , $h = \frac{D^2}{16f}$; D in terms of h and f can be calculated as

$$D = \sqrt{16hf} = 4\sqrt{hf} \quad (3.21)$$

Now putting this value of D in equation (3.20)

$$A_a = \frac{\sin\Psi}{4\sqrt{hf}}\left[34.2133\sqrt{16hf+16h^2}+136.8534f\ln\left(\frac{4h+\sqrt{16hf+16h^2}}{4\sqrt{hf}}\right)\right]\times A_r$$

$$A_a = \frac{\sin\Psi}{4\sqrt{hf}}\left[136.8532\sqrt{h(f+h)}+136.8534f\ln\left(\frac{h+\sqrt{h(f+h)}}{\sqrt{hf}}\right)\right]\times A_r \quad (3.22)$$

From the equation (3.6)

$$\tan \Psi_{rim} = \frac{\frac{f}{D}}{2\left(\frac{f}{D}\right)^2 - \frac{1}{8}}$$

Let's take $\frac{f}{D} = k$ for ease of calculation and putting this in equation (3.6) to get $\tan \Psi_{rim}$ in terms of k

$$\tan \Psi = \frac{8k}{16k^2 - 1}$$

Now From the Pythagoras theorem, the value of $\sin \Psi_{rim}$ can be calculated as:

$$\sin \Psi = \frac{8k}{\sqrt{(8k)^2 + (16k^2 - 1)^2}}$$

$$\sin \Psi = \frac{8k}{(16k^2 + 1)} \tag{3.23}$$

Now putting $k = \frac{f}{D}$

$$\sin \Psi = \frac{8\left(\frac{f}{D}\right)}{\left(16\left(\frac{f}{D}\right)^2 + 1\right)} \tag{3.24}$$

As from equation (3.21)

$$D = \sqrt{16hf} = 4\sqrt{hf}$$

Putting the value of D in equation (3.24)

$$\sin \Psi = \frac{8\left(\frac{f}{4\sqrt{hf}}\right)}{\left[16\left(\frac{f}{4\sqrt{hf}}\right)^2 + 1\right]}$$

Upon simplifying equation

$$\sin \Psi = \frac{\left(2\sqrt{hf}\right)}{h + f} \tag{3.25}$$

Now putting this value of in equation (3.22)

$$A_a = \frac{68.4266}{\left(1 + \frac{h}{f}\right)}\left[\sqrt{\frac{h}{f}\left(1 + \frac{h}{f}\right)} + \ln\left(\sqrt{\frac{h}{f}} + \sqrt{1 + \frac{h}{f}}\right)\right] \times A_r \tag{3.26}$$

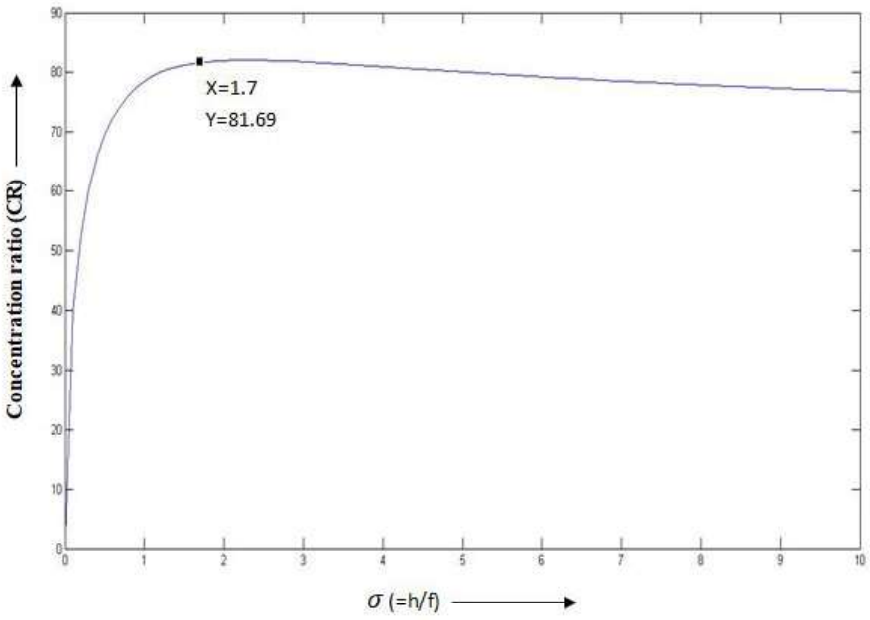

Figure 3.4: Variation of concentration ratio with $\sigma = \frac{h}{f}$

Now defining a new variable $\sigma = \frac{h}{f}$ and inserting it in place of $\frac{h}{f}$ in equation (3.26)

$$A_a = \frac{68.4266}{(1+\sigma)}\left[\sqrt{\sigma(1+\sigma)} + \ln\left(\sqrt{\sigma}+\sqrt{1+\sigma}\right)\right] \times A_r \tag{3.27}$$

$$A_a = 68.4266\left[\sqrt{\frac{\sigma}{1+\sigma}} + \frac{1}{1+\sigma}\ln\left(\sqrt{\sigma}+\sqrt{1+\sigma}\right)\right] \times A_r \tag{3.28}$$

Here A_a and A_r are related to only a single variable σ which is

$$C.R. = \frac{A_a}{A_r} = 68.4266\left[\sqrt{\frac{\sigma}{1+\sigma}} + \frac{1}{1+\sigma}\ln\left(\sqrt{\sigma}+\sqrt{1+\sigma}\right)\right] \tag{3.29}$$

Here,$C.R. = f(\sigma)$, therefore, to obtain the optimum value of concentration ratio, the differential of $C.R.$ with respect to σ must be equal to zero. $\frac{d(C.R.)}{d\sigma} = 0$ it can be seen that variation of concentration ratio with respect to σ as shown in figure 3.4. From this curve it can be seen that when $\sigma = 1.7$ value of concentration ratio is 81.69 or $\frac{A_a}{A_r} = 81.69$.

Another empirical relation between height of the parabola and its focal length is

$h = 1.7f$ and between aperture diameter, D and focal length, f is $D = 5.21f$. The value of rim angle corresponding to the optimum value of concentration ratio 81.69 is 74.97^o.

3.3 Model of the Present PTC System

Present model of PTC system includes the calculation of total length of receiver, equation of PTC, length of PTC curve and concentration ratio. It also includes the heat loss model to determine conversion efficiency of helical coil solar cavity receiver.

3.3.1 Total Length of the Helical Coil (L):

Total length of the helical coil is determined using the helical coil parameters like: total number of turns of coil (N), length of coil per unit turn (l), diameter of coil tube (d), inner diameter (D) and outer diameter (D_1) of the coil and thickness of copper tube (t) as explained below:

- **Perimeter of the copper tube** (p);

$$p = \pi \times d_i \tag{3.30}$$

- **Helical coil in one turn** (l);

$$l = \sqrt{p^2 + \pi^2 D_1^2} = \sqrt{p^2 + \pi^2 (D + d_i + 2t)^2} \tag{3.31}$$

- **Total length of the helical coil** (L);

$$L = N \times l = \left[p^2 + \pi^2 D^2 (1 + \delta + \frac{2t}{d})^2 \right]^{\frac{1}{2}} \times l \tag{3.32}$$

- **Equation and slope of parabolic trough collector**;

$$y = a \times x^2 \tag{3.33}$$

$$x^2 = \frac{1}{a} \times y, \, or \frac{1}{a} = 4 \times f = 4 \times 0.6065 = 2.426 \tag{3.34}$$

$$y = \left(\frac{50}{121.3}\right) x^2 \tag{3.35}$$

$$\frac{dy}{dx} = \left(\frac{100}{121.3}\right) x \tag{3.36}$$

where a is constant and is equal to $\frac{1}{4f}$. f is the focal length of the present PTC.

- **Length of the PTC curve** (S):

$$S = 2 \times \int_0^{0.855} \left[1 + \left(\frac{100}{121.3}\right)^2 x^2\right]^{\frac{1}{2}} dx \tag{3.37}$$

- **Concentration ratio** (CR) **of PTC system**:

$$\frac{S \times b}{\pi \times d \left[p^2 + \pi^2 D^2 (1 + \delta + \frac{2t}{d})^2\right]^{\frac{1}{2}} \times l} \tag{3.38}$$

3.3.2 Heat Loss Equation Model:

The following assumptions are made to derive the equation for PTC.

- The PTC system is operated in steady state mode.
- The heat transfer fluid, therminol VP-1 is incompressible.
- Mass flow rate of thermal oil is kept constant at any temperature.
- Viscosity of heat transfer fluid changes with time.

Energy balance equation for helical coil solar cavity receiver has been given in equation. Main challenge here is to find out the overall loss coefficient.

$$Q_u = A_h \times CR \times I_b \times \tau^n \alpha - U_t \times A_g \left(T_{gm} - T_a\right) \tag{3.39}$$

Where,

A_h=Total surface area of helical coil (m^2)

I_b= Beam solar radiation intensity of solar radiation W/m^2

τ=Transmittance of borosilicate glass

α=absorptance of receiver

A_g= Surface area of glass cover (m^2)

T_{gm}=Mean glass temperature (^oC)

T_a=Ambient temperature (^oC)

3.3.3 Conversion Efficiency Helical Coil Receiver (η_c):

The conversion efficiency is the ratio of thermal output by receiver to the sun energy input to the aperture of concentrating collector and can be calculated as:

$$\eta_c = \frac{Q_u}{I_b \times A_a} \tag{3.40}$$

$$Q_u = \dot{m} C_p (T_o - T_i) \tag{3.41}$$

Where, Q_u is the useful energy gain , I_b and A_a are the direct solar radiation intensity and aperture area respectively. T_i and T_o are the temperatures at the inlet and the exit of the receiver. $\dot{m}$ is the mass flow rate of thermal oil flowing through the helical coil and $C_p$is the specific heat capacity of thermal oil.

3.4 Experimental Analysis

Fig. 3.5 shows the schematic diagram of experimental setup installed at roof top of CERD, Mechanical Engineering Department, IIT (BHU), Varanasi. Parallel rays of solar radiations falling on the aperture of the parabola are concentrated on a helical coil solar cavity receiver which is covered with two concentric borosilicate glass tubes. The thermal oil which passes through this helical coil tube collects heat and transfers it to water in the hot water tank. The oil temperature at inlet of the absorber tube and surface temperature of the vacuum outer cell are measured by thermocouple sensors which transmit the signals to a data logging facility connected to the present setup. A sun tracker continuously tracks the sun and as a result the cycle can run efficiently. The tracker tracks the sun on

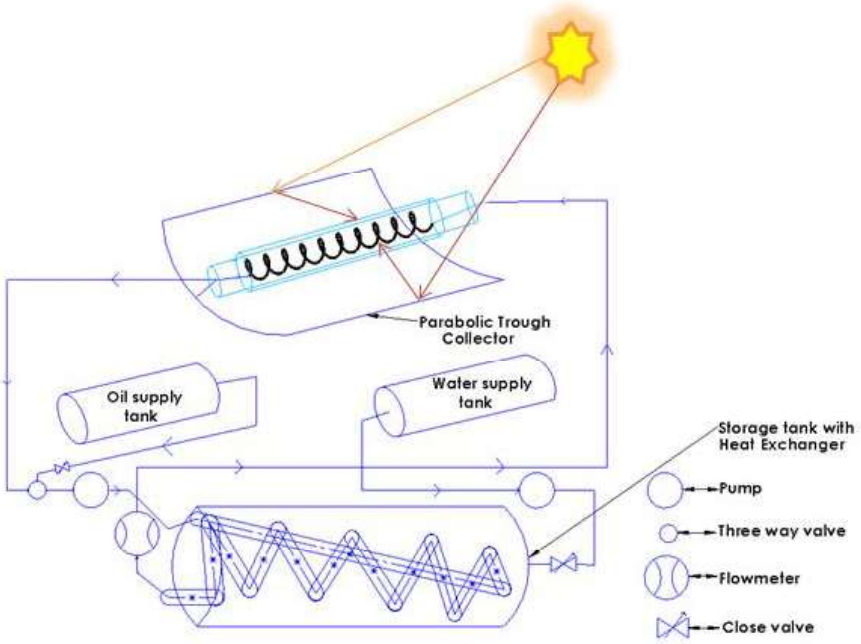

Figure 3.5: schematic diagram of line concentrating parabolic trough concentrator at CERD, IIT (BHU), Varanasi

an hourly basis by rotating the PTC at a 15° angle per hour. Figure 3.6 and Figure 3.7 shows the photograph of experimental setup used for water heating purposes and steam generation. In the setup of steam generation, water is directly heated for steam generation. Water is entered at the inlet end of helical coil solar cavity receiver and continuously passes through the line concentrating receiver where the water get heated and converted to steam. Before going through the data collection, initially experimental setup is set to be well focused and remain focused up to 30 to 40 minutes so that the receiver temperature reached up to 290^oC then water or oil is passes through the receiver coil as per our requirements. In the present linear concentrating parabolic trough collector, the concentration ratio is 19.77. Further, the data on experimental setup are collected on different days daily from January to December 2017. However, some of the collected data around the days have been used for performance analysis.

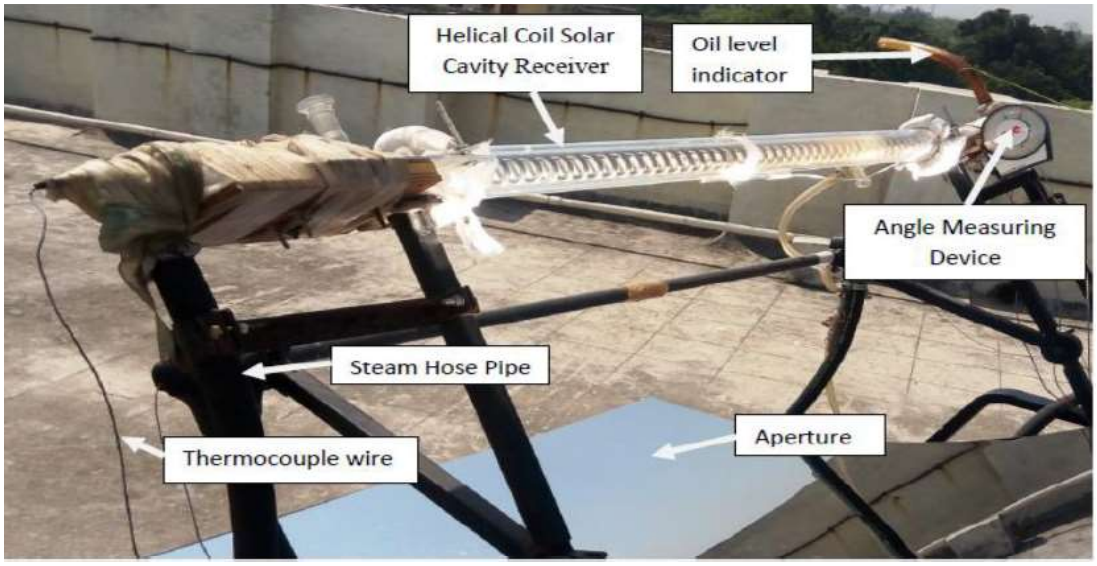

Figure 3.6: Line concentrating helical coil solar cavity receiver at CERD, IIT (BHU), Varanasi

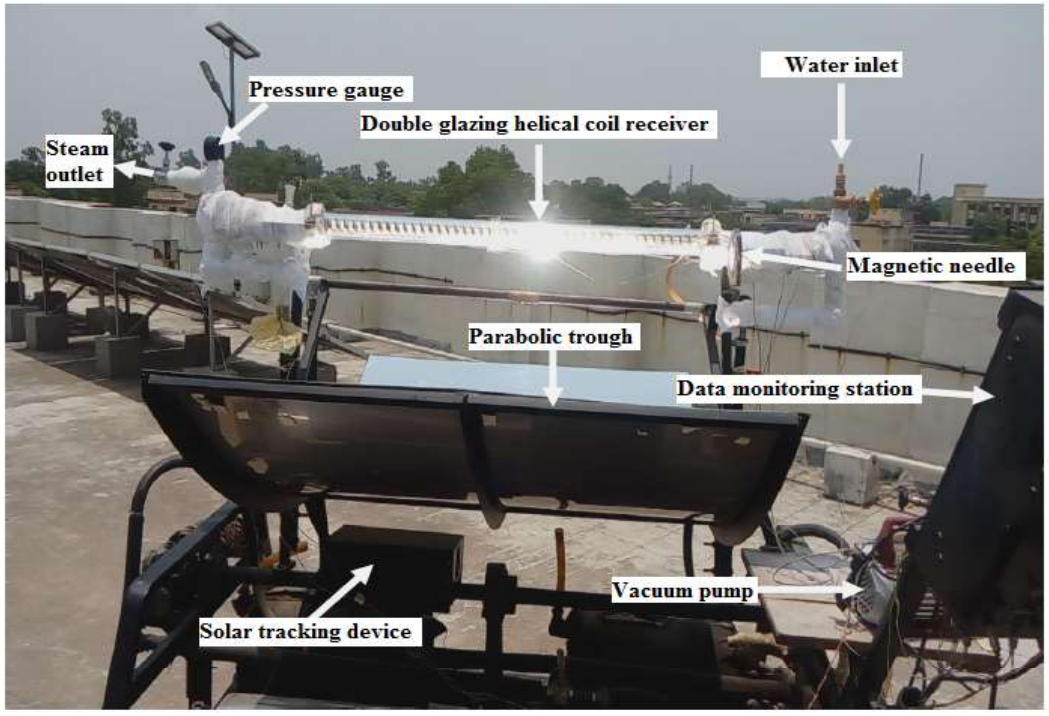

Figure 3.7: Experimental set for steam generation using helical coil solar cavity receiver at CERD IIT (BHU), Varanasi

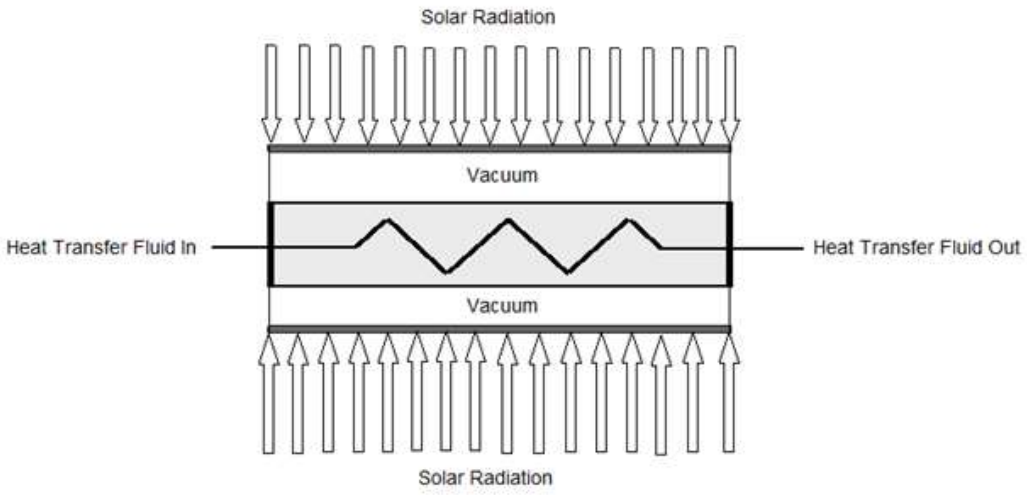

Figure 3.8: Schematic diagram of helical coil solar cavity receiver

3.4.1 Description of Receiver System

Figure 3.8 shows the schematic diagram of helical coil solar cavity receiver, kept at the focal line of parabolic trough concentrator. Helical coil tube is covered with two concentric borosilicate glass tubes with vacuum in the annulus. Solar radiation crosses the two concentric glass covers followed by vacuum level in the annulus and absorbed by blackened helical coil receiver. The heat transfer fluid utilizes this absorbed energy passes through the helical coil copper pipe whose dimensions are specified as shown in Fig. 3.9. The performance analysis of PTC system uses input parameters which are shown in Table 3.1. Helical coil tube is supported by light 'aluminium' rod by inserting it longitudinally through the coil helix diameter to avoid vertical deflections. The whole system of the receiver has been backed by support bracket which is kept at the receiver at the exact focal line of parabolic trough concentrator.

3.5 Instrumentation

In the present experimental set, two types of measuring devices was used: external devices and internal devices. External devices measure the environmental parameters like wind speed, wind direction, relative humidity, beam solar radiation, diffuse solar radia-

Table 3.1: The input parameters used in the present experimental analysis

Input Parameters used	Dimensions/Units
Length of helical coil	5.172 m
Perimeter of copper tube	0.02188 m
Receiver Area	$0.113716 m^2$
Parametric length of receiver	1.8432 m
Width of collector	1.220 m
Aperture Area	$2.2487 m^2$
Concentration Ratio	19.77
Diameter of Helical circle (D)	0.025 m
Diameter of Cu Tube(d)	0.005 m
Thickness of Cu Tube(t)	0.001 m
Pitch of Helical coil(P)	0.02438 m
Number of turns(N)	50
Gap between helical coil and 1st glass cover (Scg)	0.00125 m
Gap between 1st glass cover and 2nd glass cover(Sgg)	0.00426 m
Mass flow rate in the absorber tube	0.0882 kg/s
Wind speed	2.03 m/s
Solar radiation intensity	$600 to 900\ W/m^2$
Environmental temperature	$40.25^o C$
Density of heat transfer fluid (HTF)	$900 kg/m^2$
Thermal conductivity of HTF	0.165 W/m-K
Specific heat capacity of HTF	2061 J/kg-K
Dynamic viscosity of HTF	$0.027\ N-s/m^2$

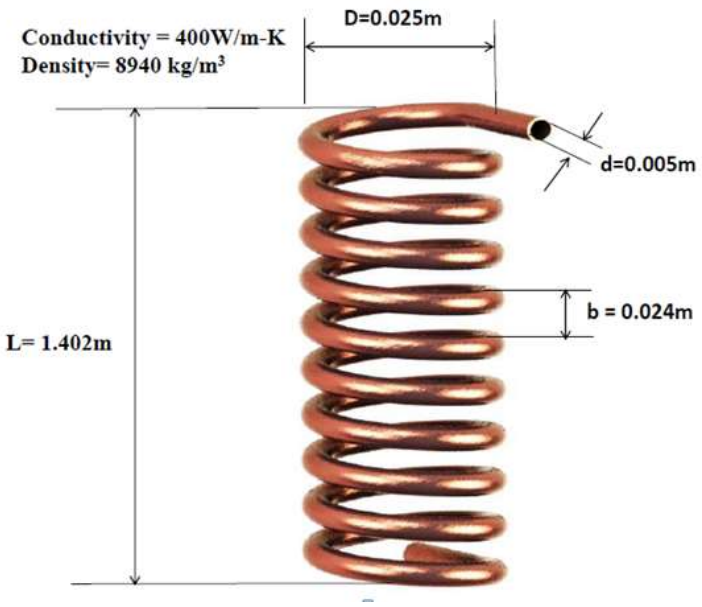

Figure 3.9: Dimensions of copper helical coil absorber tube used in PTC

tion and air temperature etc. Internal devices measure the experimental parameters like oil flow rate, tilt angle, vacumm at the annular space of helical coil receiver, temperatures at different points of receiver and oil. Overall specifications of the present experimental setup has been shown in tables 3.2 and 3.3.

3.5.1 Measurement of Experimental Parameters

Experimental parameters includes the measurement of temperature of heat transfer fluid, water and receiver at different points. It also includes the measurement of tilt angle of axis of parabolic trough collector (using magnetic needle) for giving information related to the proper tracking of the sun. Tracking was done using gear tracking mechanism and manual tracking. Vacuum created at the annular space of helical coil receiver is measured by vacuum gauge and vacuum was created using vacuum vane rotary pump of $1/3$ HP. Steam pressure was measured using steam pressure gauge fitted at the outlet of helical coil receiver. All the integrated devices used for the measurement of experimental parameters have been shown in figures 3.10, 3.11, 3.12, 3.13 and 3.14.

Table 3.2: The collective specifications of experimental setup

S.No.	Components	
	Heat energy generating system with tracking unit	Specifications
1	**Parabolic Reflector**	**Specification**
	Length	4 ft = 1.2192 m
	Arc length (perimeter)	6 ft = 1.8288 m
	Depth	0.68 ft = 0.2072
	Focal length	1.99 ft = 0.6065
	Material	SS with mirror film
	Sun Tracker	Single axis
2	**Absorber Tube**	**Specification**
	Absorber material	Copper
	Insulation material (for pipe)	PUF , Glass wool
	Piping material	GI and copper
3	**Storage Unit**	**Specification**
	Supply tanks	2 (one for water and another for oil)
	Capacity	46 ltr (for water) and 10 ltr (for oil)
	Material	SS
	Storage tank	2 (one with Heat exchanger and other without heat exchanger)
	Capacity	28 ltr
	Material	SS
	Insulation used	Glass wool with Rexene
	Tank insulation thickness	2cm = 0.02m
	Pipe insulation thickness	1cm = 0.01m
	Working fluid	Water and oil
4	**Control Unit**	**Specification**
	Pump (for water)	
	Power rating	0.1 HP = 74.57 W
	Head	6 m

Table 3.3: The collective specifications of experimental setup

S.No.	Components	
	Heat energy generating system and devices	**Specifications**
1	**Pump (for oil)**	
	Power rating	0.5 HP = 372.85 W
	Head	10 m
2	**Different Measuring Devices**	**Specification**
	RTD sensor	To measure temperatures
	Flow meter	To measure flow rate
	Hygrometer	To measure relative humidity
	Data monitoring station	To measure environmental data like solar radiation intensity, wind speed, wind direction, air temperature etc.

Figure 3.10: Photograph of circular magnetic needle to measure tilt angle of PTC

Figure 3.11: Photograph of vacuum vane rotary pump to create the vacuum at annulus

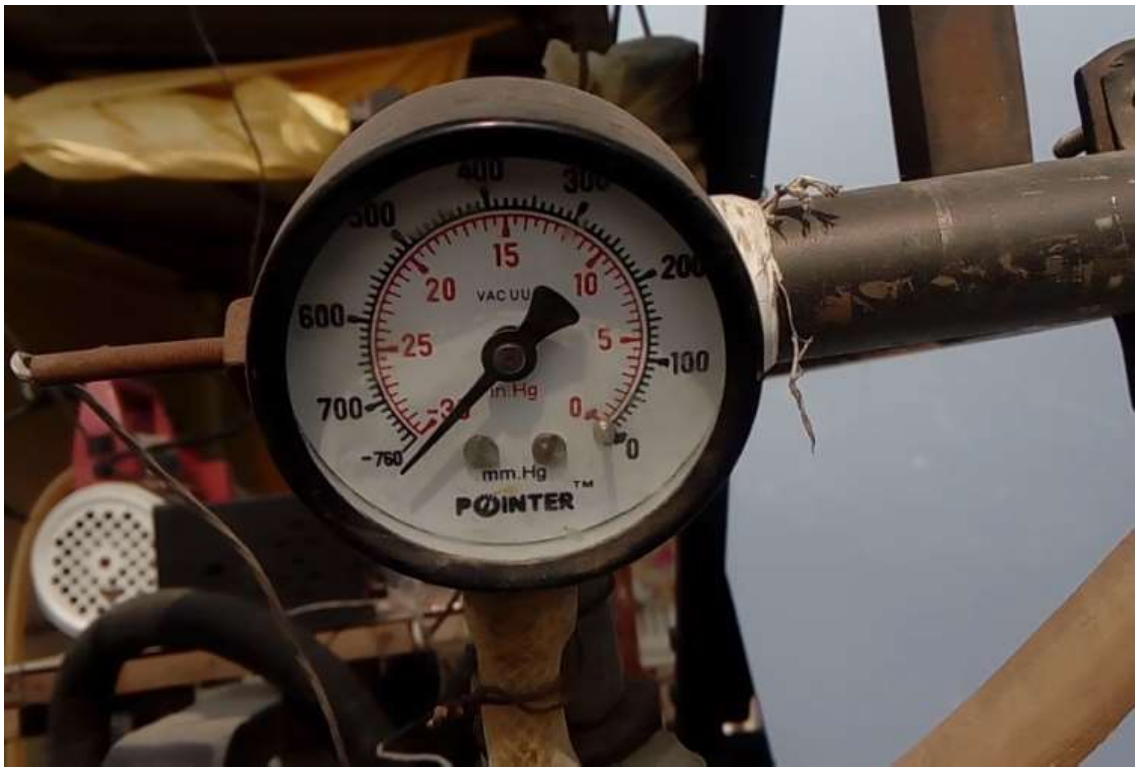

Figure 3.12: Photograph of vacuum gauge to measure vacuum pressure at annulus

Figure 3.13: Photograph of steam pressure gauge to measure steam pressure inside the helical coil

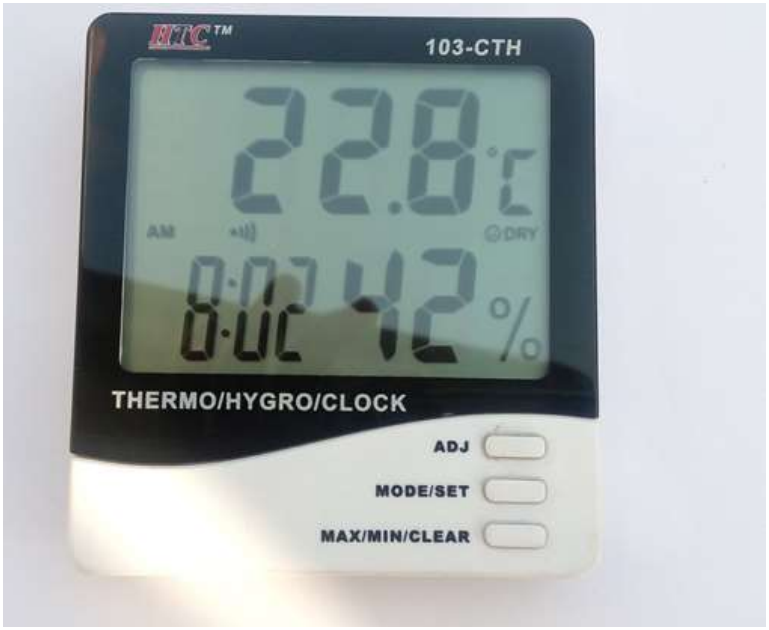

Figure 3.14: Photograph of hygrometer to measure relative humidity

Figure 3.15: Photograph of temperature indicator

3.5.2 Temperature Measurement

Present work basically deals with the heat transfer analysis of helical coil solar cavity receiver therefore, measurement of temperature is of prime importantce. Thermocouples were used to measure the temperatures at different points of the setup. A thermocouple consists of junctions at two different temperature formed using two dissimilar electrical conductors. Thermocouple basically creates potential difference between its hot and cold junction which depends on the temperature. This temperature dependent voltage is interpretated to measure the temperature. J- type thermocouple has been used in the present experimental analysis to measure the temperature after being calibrated successfully. The output of thermocouple was recorded using temperature indicatior and RTD sensor integrated with the experimental setup as shown in figure 3.15.Thermocouple wire was attached at two different points of helical coil receiver to measure the temperatures along its length. Thermocouple wire at one point has been shown in figure 3.16.

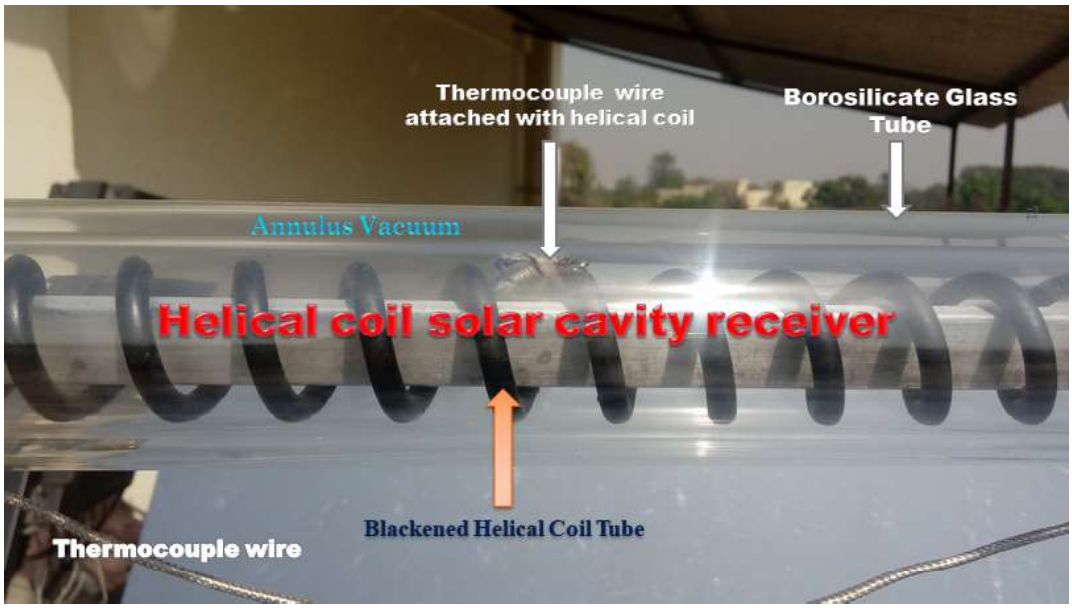

Figure 3.16: Photograph of blackened helical coil receiver with thermocouple wire attached with it

3.5.3 Measurement of Environmental parameters

Enviromental parameters like intensity of solar radiation (beam or diffufe), wind speed, wind direction, and air temperature etc. were measured using datamonitoring station installed at roof top of CERD, IIT(BHU),Varanasi as shown in figure 3.17. Solar radiation data was measured using pyrheliometer and pyranometer. Pyrheliometer consists of a collimated detector which measures beam radiation at normal incidence. Pyrheliometer is not kept at an angle of latitude of the location in question to receive solar radiation at normal incidence. Pyranometer measures the total hemispherical solar radiation on a horizontal surface. It measures global radiation i.e. sum of beam and diffuse radiation. It can also measure diffuse portion of the global radiation if shaded from the beam radiation by a shade ring or disc. Photograph of pyrheliometer and pyranometer has been shown in figures 3.18 and 3.19.

3.6 Experimental Observations

The experiment has been performed under varanasi climatic condition. The environmental data for the month of April 2017 was shown in Table 3.4 to measure the parameters

Figure 3.17: Data monitoring station to measure environmental parameters at CERD IIT(BHU), Varanasi

Figure 3.18: Photograph of pyrheliometer to measure beam radiation

Figure 3.19: Photograph of pyranometer to measure diffuse radiation

that influence the performance of solar collectors. The performance parameters under consideration have been shown in Table 3.5.

3.7 Data Reduction

3.7.1 Solar Irradiation Absorptions

The intensity of solar radiation available on the collector aperture of the present experimental setup is calculated as the product of collector aperture (A_a) and of the intensity of beam solar radiation (I_b).

$$Q_{si} = A_a \times I_b \tag{3.42}$$

3.7.2 Useful Energy Gain

The useful energy gain (Q_u) by the heat transfer fluid can be calculated in two different ways. First, using the energy balance equation in the fluid control volume as presented in eq. 3.43. The same amount of heat can also be find out using general heat transfer eq.

Table 3.4: Environmental data for the month of April 24, 2017

S.N	Time hrs.	Beam solar radiation (W/m^2)	Diffuse solar radiation (W/m^2)	Air temperature (^oC)	Wind speed (m/s)	Wind direction $^o(W-N)$	Relative humidity $(\%)$
1	08:00	514	227	32.7	1.5	242	41
2	09:00	594	236	33.1	0.7	73	41
3	10:00	765	260	34.2	0.5	170	37
4	11:00	811	279	36.4	0.7	174	39
5	12:00	790	279	38.1	1.8	37	35
6	13:00	731	267	39.6	1.2	54	26
7	14:00	610	260	40.6	1.2	179	27
8	15:00	431	223	41.9	0.4	75	22
9	16:00	127	114	40.7	1.7	102	28
10	17:00	94	94	40.5	1.9	83	28
11	18:00	19	14	39.6	0.3	77	31

Table 3.5: Experimental observations with vacuum of 10 torr at annular space of receiver for the month of April 24, 2017

S.No.	Time	Hot Water Temp. (^oC)	Absorber inlet temp. (^oC)	Absorber outlet temp. (^oC)	Absorber tube temp. (^oC)	Tank inlet temp. (^oC)	Tilt angle (in degree)	Helical coil temp. Point 1	Helical coil temp. Point 2	Supporting rod temp. (^oC)	Mass flow rate LPM	Surface Azimuth (in degree)
1	09:30	34	45	62.4	88	51.4	40	64	64	37.5	5.57	80
2	10:00	35	45.9	54.6	75	57.1	35	58	58	36.4	5.88	80
3	10:30	38.4	49.9	55.7	74	68.6	29	56	54	38.9	5.88	70
4	11:00	42	52.5	59.4	88	64.3	23	58	58	41.7	3.97	60
5	11:30	45.5	56.3	60	73	65.3	16	57	56	42.5	5.13	40
6	12:00	48.5	57.9	60.5	63	65.3	15	57	58	42.8	5.57	20
7	12:30	51.2	60.7	64.7	78	66.4	16	62	62	44	5.88	-25
8	01:00	53.5	60.2	63.7	67	66.9	24	61	62	45.7	5.88	-45
9	01:30	55.2	61.5	66.5	73	69.1	29	66	65	46.2	5.88	-72
10	02:00	57.2	64.5	66.4	69	69.5	35	62	63	47.2	5.88	-80
11	02:30	59	66.7	68.4	65	71.8	41	65	65	48	5.88	-85
12	03:00	60.5	64.6	67.2	57	70.4	48	62	62	47.7	5.88	-90
13	03:30	61.4	62.6	63.5	45	67	51	59	60	44.8	5.88	-90

3.44 between absorber to the heat transfer fluid.

$$Q_u = \dot{m} \times c_p \times (T_e - T_i) \tag{3.43}$$

$$Q_u = h \times A_{ri} \times \left(T_r - T_{mf}\right) \tag{3.44}$$

Where, $\dot{m}$= mass flow rate of oil (kg),

c_p= specific heat capacity of HTF $(kJ/kg-K)$,

T_e= temperature at the exit of helical coil tube (K),

T_i=temperature at the inlet of helical coil tube (K),

T_r=temperature of the surface of receiver tube,

T_{mf}= mean fluid temperatute(K)=$(T_i + T_e)/2$

Q_u= useful energy gain (kJ),

h=convective heat transfer coefficient between fluid receiver interface (W/m^2-K) and can be calculated using the eq. 3.45.

$$h = \left(Nu_{di} \times k_f\right)/d_i \tag{3.45}$$

h can also be calculated experimentally using the eq. 3.46

$$h = \frac{\dot{m} \times c_p \times (T_e - T_i)}{A_{ri} \times \left(T_r - T_{mf}\right)} \tag{3.46}$$

3.7.3 Calculation of Nusselt Number(Nu)

Nusselt Number can be calculated using the emperical relation suggested by Xin et al.(1997) in eq. 3.47

$$Nu = \left(2.153 + 0.318 De^{0.643}\right) Pr^{0.177} \tag{3.47}$$

with $De = Re_i \times \sqrt{\frac{d_i}{2R_c}}$; and $Re_i = \frac{\rho v_i d_i}{\mu}$;

3.7.4 Calculation of Thermal Efficiency(η)

Thermal efficiency of the system can be calculated using the eq. 3.48

$$\eta = \frac{\dot{m} \times c_p \times (T_e - T_i)}{A_a \times I_b} \tag{3.48}$$

3.7.5 Pressure Drop Calculation

Pressure drop across the length of helical has been calculated using the eqs. 3.49, 3.50 and 3.51suggested by Ito's laminar and turbulent resistance formulae (2006)

$$f_{coil} = \frac{344\left(\frac{D}{d}\right)^{-0.5}}{\left[1.56 + \log_{10}\left\{Re\left(\frac{D}{d}\right)^{-0.5}\right\}\right]^{5.33}} \tag{3.49}$$

$$\Delta P = f_{coil}\frac{L}{d}\left(\frac{1}{2}\rho v^2\right) \tag{3.50}$$

$$v = \frac{\dot{m}}{\rho\left(\frac{\pi}{4}d^2\right)} \tag{3.51}$$

Where,

f_{coil}= friction factor of the coil tube,

D= curvature diameter of the helical coil(m),

d=diameter of coil tube (m),

L= total length of the helical coil receiver(m),

ρ=density of heat transfer fluid (kg/m^3),

v=velocity of flow (m/s),

3.7.6 Mass Flow Rate Calculation $(\dot{m})$

Mass flow rate can be calculated using the eq. 3.52

$$\dot{m} = \frac{1}{60} \times \rho \times V \times 10^{-3} \tag{3.52}$$

Where,

ρ=density of HTF $(900\ kg/m^3)$,V= volume flow rate of oil (5.88 LPM)

3.8 Experimental Results

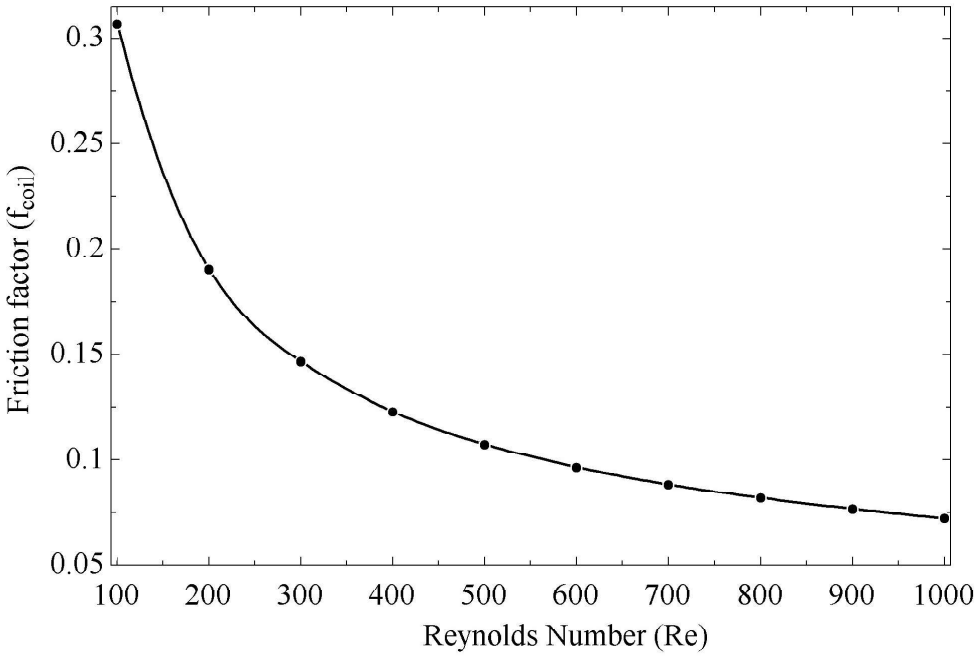

Figure 3.20: Variation of friction factor with Reynolds number for helical coil tube

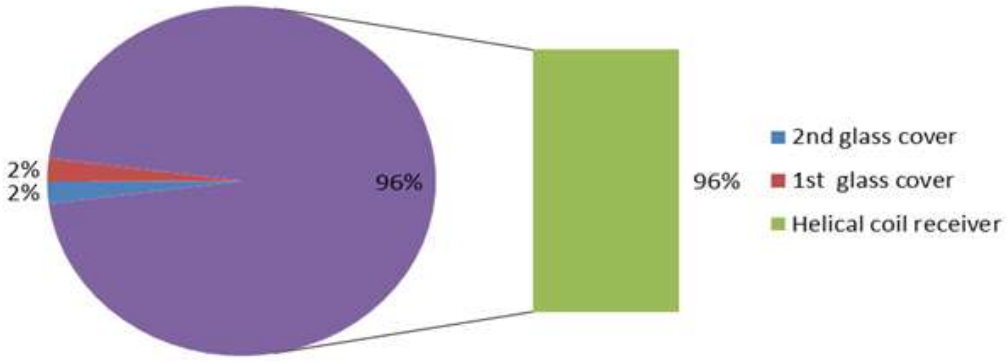

Figure 3.21: Solar irradiation absorptions by receiver, 1^{st} glass cover, and the 2^{nd} glass cover

The helical coil solar receiver was covered with two concentric glass cover with vacuum at outer annulus. The amount of solar radiation absorbed by receiver, 1^{st}glass cover and 2^{nd}glass cover has been shown in figure 3.21. It is clear that the maximum portion of solar radiation was absorbed by the receiver tube while the glass covers absorbs only 2% of the

total solar radiation incident on it. In the present experimental work this type of solar radiation absorption phenomena is of prime importance. The borosilicate glass is used to cover helical coil due to its high transmitivity and heat resistant properties. Comparison of performance of straight tube receiver with helical coil tube receiver has been depicted in figure 3.6. It shows how the helical coil receiver is beneficial over horizontal tube receiver. Convective heat transfer coefficient is higher for helical coil receiver in comparison to straight tube due to secondary flow which arises due to the flow of fluid through the curve pipe. Variation of thermal efficiency and convective heat transfer coefficient was shown clearly in Table 3.7. In this table, convective heat transfer coefficient and thermal efficiency for the different experimental data has been calculated and it was found that the maximum value of thermal efficiency achieved is 86.53% . Variation of friction factor and pressure drop across the length of helical coil with reference to the Reynolds Number (Re) and velocity of flow of heat transfer fluid respectively were shown in figures 3.20 and 3.22. It shows clearly that pressure drop across the length of helical coil increases as the velocity of flow of heat transfer fluid increases. At higher mass flow rate power consumption is higher. At the same time, friction factor decreases with Reynolds Numbers. Reynolds Number depends upon the the viscosity of flowing fluid through the pipe and viscosity is the function of temperature. Hence, at higher temperature low pumping power is required because of its low viscosity.

Table 3.6: Comparison straight tube receiver versus helical coil tube receiver

S.No.	Parameters	Horizontal tube receiver	Helical coil solar receiver	Units
1	Convective heat transfer coefficient(h)	407.9	766.7	W/m^2-K
2	Mass flow rate $(\dot{m})$	0.0882	0.0882	Kg/s
3	Reynolds number(Re)	180.8	831.9	Dimensionless
4	Prandtl number(Pr)	373.3	373.3	Dimensionless
5	Receiver surface area(As)	0.1034	0.1046	m^2
6	Thermal oil velocity(v)	0.2353	4.99	m/s
7	Direct solar radiation intensity(I)	917	840	W/m^2

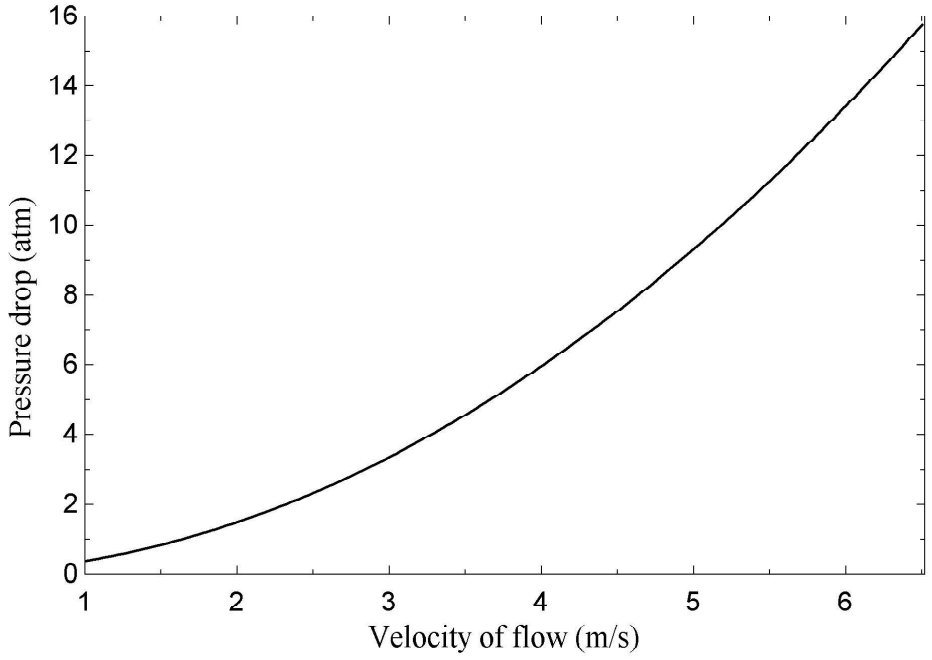

Figure 3.22: Pressure drop across the length of helical coil tube with the velocity of flow

Table 3.7: Convective heat transfer coefficient and thermal efficiency of helical coil tube

Time hrs.	Inlet Temp. $T_i,(K)$	Exit Temp. $T_e,(K)$	Receiver Surface Temp. $T_s,(K)$	Mean fluid Temp $T_m,(K)$	Beam radiation I_B (W/m^2)	Aperture area A_a (m^2)	Mass flow rate$(\dot{m})$ (kg/s)	specific heat capacity c_p $(J/kg-K)$	Useful heat gain Q_u (J)	Convective heat transfer coefficient (h) (W/m^2-K)	Thermal efficiency η_{th}
9.5	53.3	61.5	67.5	57.4	766	2.249	0.0882	2061	1491	1298	0.8653
10	66.9	68.1	70	67.5	815	2.249	0.0882	2061	218.1	767.4	0.119
11	69.9	74	76.5	71.95	862	2.249	0.0882	2061	745.3	1441	0.3844
11.5	72.8	76.7	78.5	74.75	863	2.249	0.0882	2061	708.9	1663	0.3653
12	70.9	74.7	78	72.8	863	2.249	0.0882	2061	690.8	1168	0.3559
12.5	71.1	75.2	78	73.15	840	2.249	0.0882	2061	745.3	1352	0.3945
13	72.7	76.8	80	74.75	780	2.249	0.0882	2061	745.3	1249	0.4249
13.5	75.7	76.6	77	76.15	729	2.249	0.0882	2061	163.6	1693	0.09979

Table 3.8: Uncertainties in the experiment

Measured parameters	Uncertainty
Mass flow rate	0.0960
Ambient temperature	0.0590
Concentration ratio	0.0270
Parametric length of collector	0.0076
Aperture area of PTC	0.0085
Solar radiation intensity	0.1700
Wind speed	0.5700

3.9 Uncertainty Analysis

A complete uncertainty analysis is performed on the experimental data on April 24, 2017 as shown in appendix as mentioned at the end of the thesis. The analysis takes into account the uncertainties in measured parameters like mass flow rate of heat transfer fluid, ambient temperature, concentration ratio, parametric length of collector, aperture area of PTC, solar radiation intensity and wind speed as shown in Table 3.8. The uncertainty associated with aperture area is 2.23 ± 0.01903. Hence, using the eq. 3.55 and eq. 3.56 the uncertainty associated with concentration ratio is found to be 19.77 ± 0.54.

$$R = f(X_1, X_{2,} X_3 \ldots\ldots\ldots X_N) \tag{3.53}$$

Where, R is any function of variable X.

$$\sigma_R = f(\sigma_{X_1,} \sigma_{X_2} \ldots\ldots\ldots \sigma_{X_N}) \tag{3.54}$$

where, $\sigma_R = Uncertainty\, in\, R$

$$\sigma_R = \sqrt{\sum_{i=1}^{N} \left(\frac{\partial R}{\partial X_I} \partial X_i \right)^2} \tag{3.55}$$

$$U_R = \pm \sqrt{\frac{1}{R^2}\left(\sum_{i=1}^{N}\left(\frac{\partial R}{\partial X_I}\partial X_i\right)^2\right)} \tag{3.56}$$

Where, $U_R = Relative\,Uncertainty$

This chapter discussed about the data analysis of experimental results. This chapter also includes the mathematical formulation which presents the foundation of design of criteria. Numerical modeling and validation of performance model with the experimental results has been mentioned in chapter-4.